Two associated limestone slabs with scattered bone material from the Vossenveld Formation.

State-of-the-art: virtual palaeontology of Vossenveld fossils

U vindt een samenvatting aan het eind van de tekst.

Dennis F. A. E. Voeten*[1,2] and Richard de Haan[2]
*dennis.voeten@naturalis.nl

[1]Naturalis Biodiversity Center, Leiden, the Netherlands

[2]Workgroup Muschelkalk Winterswijk, Dutch Geological Society, Winterswijk, the Netherlands

Abstract | **Ongoing improvement of tomographic visualisation techniques has sparked a digital revolution in palaeontological research by providing increasingly powerful tools for the visualisation and study of fossil remains. Here, we provide a concise overview of the history of radiography and tomography, discuss several palaeontological applications of tomographic techniques, and present published examples in which tomographic evaluations aided in the description and study of Vossenveld fossils. Finally, we demonstrate the nondestructive yet three-dimensional exploration of vertebrate fossils in the micrite matrix from the Winterswijkse Steengroeve using a medical tomograph. This case study assessed the potential presence of cranial material in limestone blocks containing diagnostic postcranial**

material of a thus far poorly known basal pistosauroid from the Vossenveld Formation. Although no obscured skeletal elements were encountered in the matrix, our study offers a clear example of the tomographic visualisation of vertebrate fossils in general, and those in the Vossenveld Formation in particular.

Tomography

X-ray radiation – Towards the end of the 19th century, a radiographic accident led Wilhelm Röntgen to the discovery of X-ray radiation (Röntgen, 1896). He observed that an electron-discharge tube produced this then-unknown type of radiation because it excited his fluorescent screen and caused it to give off visible light. Röntgen subsequently found that a lead tube placed between the X-ray source and the fluorescent screen blocked the X-rays. Moreover, he also noticed that the bones inside the hand holding this tube had the same effect. Because the bones in his hand blocked substantially more radiation than the surrounding flesh, his hand skeleton emerged as a distinct radio shadow (Frankel 1996). Shortly after his discovery, Röntgen managed to record the now famous first radiograph of his wife's hand, wearing a wedding ring, on photographic film (Jakubek, 2007).

Radiography – Radiography relies on the capacity of certain types of radiation to penetrate and traverse a diverse array of materials and visually opaque objects (e.g. Eisenberg, 1992; Kak *et al*., 2001; Hsieh, 2015). When an X-ray beam passes through an inhomogeneous object, the different media (i.e. materials) composing the object will absorb X-ray photons to different degrees. This differential attenuation can be visualised by placing the object of interest between an X-ray source and an X-ray detector. The resulting image (i.e. radiograph) maps the relative distribution of media with different X-ray absorbent properties as radiodensity shadows that can be captured on photographic film or stored as digital imagery. Projectional radiography creates a single radiograph that visualises the radiodensity shadow of an object along a single direction. Various medical applications of this method exist. We now know that calcium efficiently absorbs X-rays, making bones clearly discernible in radiographs. This helpful property was crucial in Röntgen's 1895 pioneering discovery and continues to be exploited in, for example, the recognition and assessment of bone fractures by medical specialists.

Computed tomography – Advances in digital imaging techniques allowed for computed tomography (CT) to make its first appearance in the beginning of the 1970s. CT calculates a single, three-dimensional volume from a multitude of digital radiographs through the concept of the inverse Radon transform (Radon, 1917). To achieve this, typically either the sample or the tomographic gantry is rotated while numerous radiographs are recorded. Together, these so-called projections contain all the information required for reconstructing a three-dimensional virtual model of the sample in which relative radiodensity is proportionally expressed in ascending grey levels assigned to individual voxels (i.e. 3D pixels). The quality and magnification of tomographic data is determined by properties of the radiation source, detector setup, reconstruction algorithm, and post-processing solutions. The created volume is completely continuous, obtained nondestructively, and can be shared, manipulated, and studied in absence of the physical sample itself (Rahman *et al*., 2012).

Following reconstruction, the tomographic data set exists as a stack of images that captures the radiodensity distribution within the sample along one direction through sequential cross-sectional slices. Designated software packages for CT data visualisation and analysis, such as VGStudio MAX (Volume Graphics, Heidelberg, Germany), Amira/Avizo (FEI Company, Hillsboro, United States), and Mimics (Materialise NV, Leuven, Belgium), are used for processing tomographic image stacks. These programs employ interpolation algorithms that enable data presentation in any desired orientation and appropriate field of view. The sample can be readily explored through virtual cross sections, often in multiple perpendicular views at the same time, thereby enabling evaluation of the data set and observation of phenomena in cross section. A standardised tomographic data environment for (mostly) medical applications is offered by the DICOM (Digital Imaging and Communications in Medicine) protocol, which is associated with optimised hardware, data, software, and storage solutions that guarantee universal compatibility and safeguard data identification across institutes.

Features of interest, typically characterised by a shared radiodensity and/or morphological unity, can be virtually extracted with a process called segmentation. Segmentation isolates discrete components of the sample, such as a fossil bone inside the host matrix, for spatial appreciation and analysis. Volume thresholding separates voxels within a predetermined grey-value range from voxels outside that range. This method of volume visualisation and segmentation is particularly efficient when isolating elements with a unique radiodensity signature within the sample, such as a compact fossil in a matrix of lower density. A sample containing selected elements that share their radiodensity range with trivial features within the same sample, such as specific bones in a compact bone bed or in a matrix with similar properties, may be virtually extracted through region growing algorithms. Segmentation by region growing progressively expands the region of interest following predetermined boundary conditions, which typically represent static or dynamic grey-level ranges. Not unlike the well-known 'Magic Wand' function in Adobe Photoshop, region growing starts with a selected voxel that is representative of the element under consideration. Depending on the mode of region growing, the region of interest is allowed to grow and incorporate adjacent voxels falling within a predetermined static grey level range applied to the original (seeding) voxel, or dynamic ranges based on either the adjacent (non-seeding) voxels or average values for the growing region of interest itself. In complex volumes or those presenting tomographic imperfections (artifacts) or low contrast between features of interest and the surrounding matrix, regions of interest may be segmented manually by tracing focal elements through consecutive slices. Segment-

ed regions of interest become available independently from the tomographic volume for visualisation, storage, sharing, and study. These regions of interest can furthermore be animated in 3D or exported as surface models compatible with external applications, including those enabling three-dimensional modelling, quantification, analysis, and printing.

Virtual palaeontology

Tomography in palaeontology

Computed tomography has revolutionised paleontological research. The anatomy of some fossil taxa is now better characterised than those of their living counterparts (Cunningham *et al*., 2014). Even the visualisation and three-dimensional reconstruction of delicate organs from fossilised soft tissues has entered the realm of possibility (e.g. Pradel *et al*., 2009; Eriksson *et al*., 2012; Trinajstic *et al*., 2013; Maldanis *et al*., 2016; Qvarnström *et al*., 2017; Lautenschlager 2017). The theoretical maximum resolution of synchrotron microtomography, facilitated by particular properties of a synchrotron light source, now rivals that of optical microscopy (Sanchez *et al*., 2012). Tomographic data acquisition of lithified fossils is nondestructive and thereby grants access to internal structures of valuable fossils unavailable for invasive sampling (Tafforeau *et al*., 2006). The retained integrity of these specimens furthermore ensures complete reproducibility of such studies and preserves the sample for future evaluation when improved tomographic techniques become available. Tomographic opportunities for vertebrate palaeontology include the nondestructive reconstruction of challenging skeletal fossils partially preserved in matrix (e.g. Neenan *et al*., 2013), the visualisation and interpretation of bone microstructures with virtual osteohistology (e.g. Sanchez *et al*., 2012), and the study of fossil brain shapes through cranial endocasts (e.g. Voeten *et al*., 2018). Palaeontological tomography furthermore allows for non-invasive forensic evaluation of potentially suspect material (e.g. Cau *et al*., 2017). Despite the clear advantages of virtual palaeontology, certain informative properties of fossils, such as those expressed in colour or under polarized light, cannot (yet) be visualised with tomography. Palaeontological research involving tomographic data is therefore best practiced by the complementary consideration and exploitation of particular benefits granted by traditional investigation techniques.

Tomography of Vossenveld fossils –The description of the stem placodont *Palatodonta bleekeri* by Neenan *et al*. (2013) relied on one of first tomographic evaluations of a fossil from the Vossenveld Formation. The small (20.5 mm long) and partially disarticulated cranium of a juvenile specimen could not be safely freed from the limestone matrix. Computed tomography was capable of visualising obscured morphological characters of *Palatodonta* and thereby enabled reconstruction of its cranial anatomy. Important parts of the dentition were revealed and described from tomographic data, including the row of narrow and pointed palatine teeth that is ancestral to the crushing dentition of

MORPHOLOGICAL DESCRIPTIONS OF SELECTED RDH ELEMENTS

Mandibular fragment – A gracile left mandibular fragment measuring circa 52 mm in preserved (anteroposterior) length is exposed in lingual view (Fig. 2B). Although the fragment must span several mandibular elements, the state of preservation does not allow for confident recognition of sutures separating these bones. The mandibular fragment will therefore be described as a single morphological unit.

The fragment is anteriorly delimited by a fracture that potentially corresponds with the original suture between the dentary and the angular or (anteriormost) articular. However, dorsal and medial aspects of the mandibular fragment anterior to the ex situ tooth appear damaged as well, rendering conclusive identification and assessment of dental arrangement problematic. Posterior to the tooth, a distinct trough obliquely traverses the dorsomedial mandibular ramus in an anterolateral-posteromedial direction to posteriorly terminate in the craniomandibular articulation. At this level, a robust medioventral bulge causing a distinct bend in the ventral ramal delimitation supports a saddle-like mandibular hinge in the dorsal ramus, which is anatomically associated with the angular. A coranoid process appears absent. The retroarticular process is low and slender, granting it a more cylindrical shape than the mediolaterally compressed retroarticular processes in sympatric *Anarosaurus* (e.g. Klein, 2009, Fig. 6) and *Nothosaurus* (e.g. Albers & Rieppel, 2003, Figures 3 and 4). Furthermore, the retroarticular process appears to trend somewhat posterodorsally before terminating in a slightly damaged retroarticular tip, which may oppose the more posterior to posteroventral orientation of this process in *Anarosaurus* (e.g. Klein, 2009, Fig. 6) and *Nothosaurus* (e.g. Albers & Rieppel 2003, Figures 3 and 4). The mandible in various tetrapods, such as *Nothosaurus* (Rieppel 2000), includes a laterally projecting surangular shelf that provides attachment for the superficial jaw adductor musculature. Although lateral aspects are obscured in the mandibular fragment described here, a modest lateral bulge is resolved in CT data (Fig. 3), which may serve homologous muscle attachment.

Isolated tooth –A single ex situ tooth, measuring circa 6 mm in total length, is preserved in close association with the dorsal mandibular fragment (Fig. 2A). The crown is circa 2 mm long and has a slightly swollen but generally conical and probably slightly recurved morphology. No pronounced longitudinal striations are observed on the crown, which is set off from the root by a subtle but distinct constriction. The root has a bulging cylindrical to ellipsoid shape that is coronally truncated by the crown and apically terminates in a well-developed large apical foramen. This geometry appears most consistent with a thecodont implantation. The coronal 20% of the root length remains covered with enamel whereas the apical 80% of the root is covered with cementum.

Scapulae –Both scapulae recall the conditions described for another pistosauroid assemblage and partial skeleton described from the Vossenveld Formation (Sander *et al*., 2014). As such, they involve a broad, ventrally expanded portion and a slender, posterodorsally trending scapular process (Figures 2 and 3). The anterior to medial scapular margin is rounded whereas the lateral margin is relatively straight and continues onto the lateral scapular blade. A distinct ventral crest emerges near the anterior scapular margin and descends posteriorly to an angular bulge positioned near the posterior scapular margin. This crest divides an anteroventral facet from a ventromedial facet. Although the ventral scapula is overall convex, these individual facets are slightly concave.

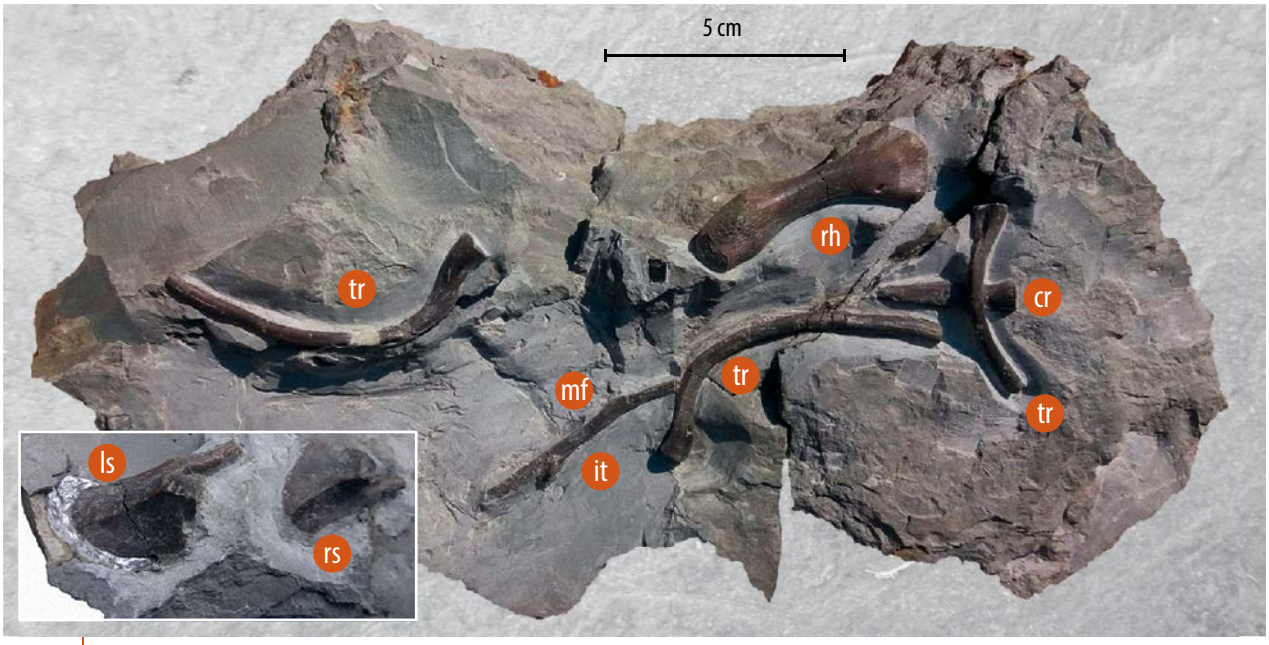

FIGURE 1. | *Association of vertebrate elements from the Vossenveld Formation at the Winterswijkse Steengroeve. Most elements are contained on Slab 1 (main image) whereas the two scapulae are preserved on Slab 2 (inset). Abbreviations – cr: caudal rib, it: isolated tooth, ls: left scapula, mf: mandibular fragment, rh: right humerus, rs: right scapula, tr: thoracic rib.*

placodonts (Neenan *et al*., 2013). A study by Klein *et al*., (2015) presented numerous postcranial associations of *Nothosaurus marchicus* from the Vossenveld Formation, some of which reside in private collections. Several casts were manufactured to retain representative references of this material in the public collection of the Steinmann

At the apex of the ventral bulge, the posteroventrally trending crest bifurcates into a short posterodorsally ascending ridge terminating at the posterior scapular margin and a short laterodorsally ascending ridge that terminates at the scapular process. This results in a descended, roughly squared facet on the posteroventral scapula that would have communicated with the coracoid during life. In posterior view, a fan-shaped articular facet pointing downwards represents the glenoidal contribution of the scapula. Medially, this facet borders a small notch in the posterior scapular margin. The scapular process has an overall straight, subconical shape. In both scapulae, the posteriormost tip is missing. The preserved anteroposterior lengths of the left and right scapula are 40 and 36 mm, respectively. The geometries of scapular processes in Vossenveld Sauropterygia in general, and in putative pistosauroids in particular, is known to be subject to yet unexplained shape variation (Oosterink *et al*., 2003; Sander *et al*., 2014). The processes on both scapulae described here appear to include a small but noticeable 'kink' at their base that, particularly in the left scapula (Fig. 2C), appear to results from a lateral concavity at the level of a medial bulge. Although dorsal aspects of both scapulae remain obscured, CT data indicates that the dorsal scapular surface forms a relatively uniform concavity (Fig. 3), as in other Vossenveld pistosauroids (Sander *et al*., 2014).

Humerus –The well-preserved right humerus measures circa 55 mm in total length and is prepared in dorsal view (Fig. 2D). Maximum dimensions of the proximal and distal head measure 14 and 20 mm, respectively, whereas the mid-diaphysial constriction measures only 7 mm. The proximal humerus carries a low dorsal ridge that proximally terminates in a slight dorsal expansion of the humeral articular head and distally descends into the smooth humeral shaft. This ridge separates two rugose facets and likely represents the *crista tuberculi minoris* that served as the humeral attachment for the *musculus latissimus dorsi*. The postaxial humeral head carries several longitudinal striations. Distally to the dorsal ridge, the humeral diaphysis tapers to a very smooth, constricted mid-diaphysis with a relatively circular cross section. Distal to the mid-diaphyseal constriction, the shaft again broadens towards the distal humeral head, granting the humerus a distinct hourglass shape. With its diverging pre- and postaxial margins, the dorsoventrally compressed distal humeral head exhibits a profoundly 'flared' geometry. A distinct ectepicondylar groove separates the proximally retracted capitulum on the preaxial distal head from the pronounced distally-projecting ectepicondyle. The distal humeral facet continues postaxially towards and onto the entepicondylar bulge. More proximally, the transition from the smooth diaphyseal shaft to the entepicondyle is marked by a semicircular entepicondylar foramen. As such, the characteristic humeral morphology agrees with those for the basal pistosauroid (?*Cymatosaurus*) described from the Vossenveld Formation by Sander *et al.* (2014), which was earlier believed to represent *Dactylosaurus* sp. (Oosterink *et al*., 2003).

In comparison to the pistosauroid associations from the Vossenveld Formation of Winterswijk described by Sander *et al.* (2014), the left scapula and right humerus described here are between 12% and 30% smaller than corresponding elements in respectively RGM 445912 (scapula) and RGM 449487 (humerus). These previously described associated elements all exhibit a humerus/scapula length ratio of 1.6 (Sander *et al*., 2014). The humerus/scapula length ratio in the RdH association, as obtained through the proximodistal length of the right humerus (55 mm) and the anteroposterior length of the left scapula (40 mm), is about 1.4. This discrepancy may stem from taxonomic or ontogenetic variation, or represent sexual dimorphism.

Institute (University of Bonn, Bonn, Germany). However, physical casting of one specimen (JLW 300, composed of two slabs) proved impossible without risk of damaging the fossil. Micro-CT scans of JLW 300 were therefore secured to allow for later corroboration and assessment. Zuber *et al.* (2017) demonstrated the complementary advantages of CT and computed laminography (CL) for visualising diagnostic features in a compressed (i.e. flattened) horseshoe crab fossil from the Winterswijkse Steengroeve.

CT data acquisition of large and oblate (i.e. plate-like) fossils suffers from the thickness variation encountered during sample rotation in the X-ray beam. Where conventional CT typically sees rotation of the sample around an axis perpendicular to the X-ray beam direction, CL introduces a laminographic angle to reduce sample thickness in the X-ray path and thereby improves image quality for certain domains in the sample (Zuber *et al.*, 2017). Exploitation of the complementary benefits of CT and CL through the newly introduced method of augmented laminography (AL) allowed for classification of the Vossenveld horseshoe crab as the genus *Limulitella* (Zuber *et al.*, 2017). Voeten *et al.* (2018) employed synchrotron microtomography for visualising the internal anatomy of a *Nothosaurus marchicus* cranium from the Vossenveld Formation. This endocranial exploration encountered progressive adaptations to secondary marine life, including nasal glands exapted as salt glands and an atrophied accessory olfactory system. However, *Nothosaurus marchicus* was also found to exhibit niche-optimised conditions, such as profound straightening of the brain resulting from constriction by the snapping temporal musculature. *Nothosaurus marchicus* was concluded to have been a piscivorous visual ambush predator in shallow marine habitats with a life position near the seafloor and a likely exothermic thermal strategy.

Case study: visualising a vertebrate assemblage from the Winterswijkse Steengroeve using a medical CT scanner

Materials –The assemblage presented here (Fig. 1) is housed in the collection of RdH. It was encountered in Layer 10

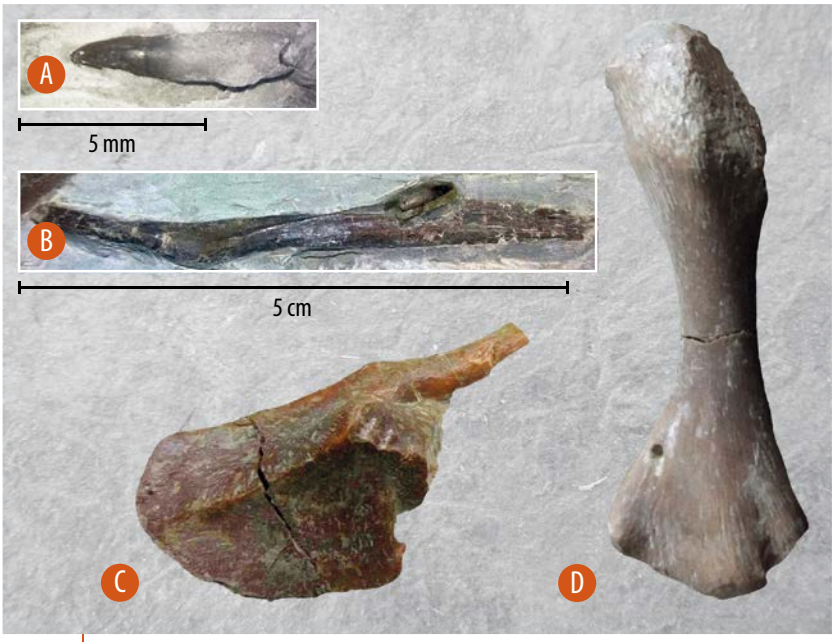

FIGURE 2. | *Selected elements of the RdH association. A. Isolated tooth (scale bar 5 mm). B. Mandibular fragment with isolated tooth, C. Pistosauroid left scapula, D. Pistosauroid right humerus (scale bar B-D 5 cm).*

(Oosterink, 1986) on 20 June 2015 and salvaged in two rock slabs containing multiple skeletal elements. The assemblage has also been considered in a recent study focusing on the taphonomy of the Vossenveld Formation (Heijne *et al.*, 2019).

Mechanical preparation has revealed a partial left mandibular ramus, three thoracic ribs (including a partial rib), a caudal rib, two bilateral scapulae, a left humerus, a tooth, and a ganoid fish scale. The scapular and humeral morphologies enable confident identification as Pistosauroidea (aff. *Cymatosaurus*). Although pistosauroid postcranial material is known from the Vossenveld Formation (Oosterink *et al.*, 2003, then considered *Dactylosaurus*; Klein, 2010; Sander *et al.*, 2014; Voeten *et al.*, 2015), corresponding cranial material has thus far not been recognised in these deposits.

The poorly preserved mandibular fragment and closely associated but disarticulated tooth in the association exhibit morphological characters inconsistent with Pistosauroidea known from other Middle Triassic deposits. These elements furthermore disagree with those of the locally common sauropterygian genera *Nothosaurus* and *Anarosaurus*, and may potentially even represent fish rather than amniote fossils. Nevertheless, the presence of a mandibular fragment of unknown affinity in close association with at least three pistosauroid elements fueled an investigation into the potential presence of additional associated cranial material inside the two slabs. To scout the rock matrix for additional elements without risking damage to already exposed bones, the slabs were subjected to a tomographic assessment. A detailed morphological description of the referred mandibular fragment, tooth, scapulae, and humerus (Fig. 2) is provided in the orange inset.

Methods –A tomographic experiment was conducted on 21 December 2016 at Isala Diaconessenhuis in Meppel (the Netherlands). The micritic slabs preserving the fossil assemblage were visualised (Fig. 3) using an Aquilion PRIME CT scanner with a slice thickness of 0.5 mm and an x-y plane spatial resolution of 0.39-0.45 mm. At a tube potential of 120 kV, average photon energy was approximately 70 keV. The obtained scan data were explored and segmented using VGStudio MAX 2.2 (Volume Graphics, Heidelberg, Germany).

Tomographic exploration –No additional elements were encountered in the rock slabs. Nevertheless, the presented experiment did demonstrate that skeletal fossils (partially) encased in a micritic matrix from the Vossenveld Formation can be

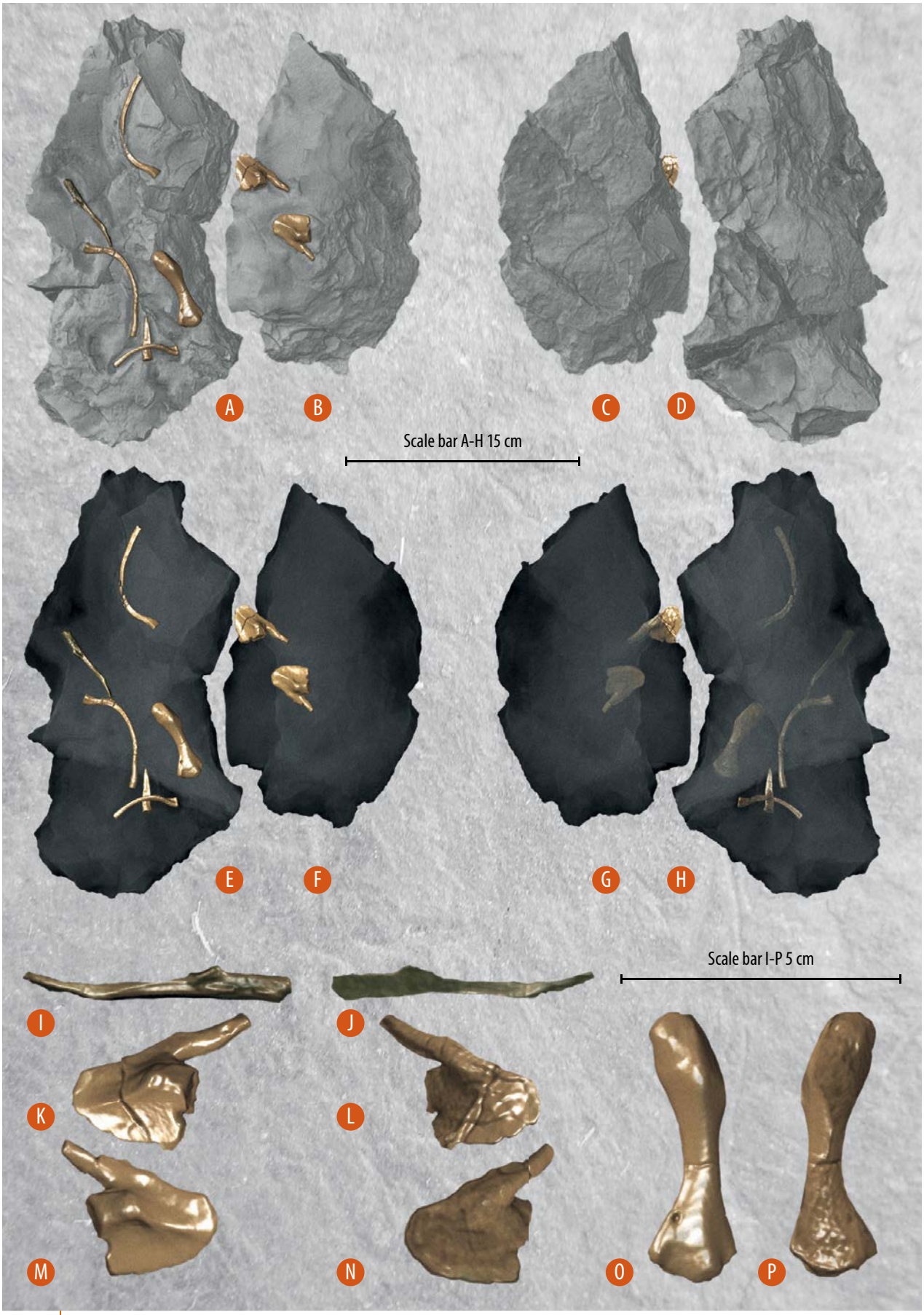

FIGURE 3. | *Digital renderings of RdH association. A-D. Surface renderings of Slab 1 (A,D) and Slab 2 (B,C) in top (A,B) and bottom (C,D) view. E-H. Semi-transparent renderings of Slab 1 (E,H) and Slab 2 (F,G) in top (E,F) and bottom (G,H) view with segmented skeletal elements. I-J. Mandibular fragment in medial (I) and lateral (J) view. K-L. Left scapula in ventral (K) and dorsal (L) view. M-N. Right scapula in ventral (M) and dorsal (N) view. O-P. Right humerus in dorsal (O) and ventral (P) view.*

successfully visualised using medical tomographs. Although smaller details, such as the geometry of the isolated tooth, could not be reliably resolved, scanning resolution and contrast proved sufficient for visualising obscured macromorphological features. The mandibular fragment is too thin to provide reliable morphological or geometrical information with the used method, rendering its affinity unknown for now.

Conclusions

Tomographic visualisation techniques present valuable opportunities for the study of palaeontological material. These applications, colloquially referred to as 'virtual palaeontology', exploit particular benefits that tomography has to offer over more traditional approaches. Virtual palaeontology is nondestructive, completely continuous in three dimensions, and makes representative data available independently from the fossils they represent. Accelerated development of tomographic methods, such as the continuously increasing resolution and contrast of synchrotron imaging and the improved visualisation of flattened fossils using laminography, will consolidate the role of tomography in palaeontological research by enabling research that was previously impossible or substantially more demanding. Improved access to tomographic equipment and facilities will aid in the broad adoption of virtual palaeontology. The value of tomography in the study of fossils from the Vossenveld Formation is exemplified by several studies that will inspire future explorations of this material. Although the case study presented in this report did not reveal cranial material of conclusive pistosauroid affinity, it did indicate that approachable tomographic techniques already offer powerful tools for the non-destructive exploration of potentially fossil-bearing Vossenveld micrite slabs.

Acknowledgements

We are very grateful to Tanja de Ruiter-Weide, Hellen de Vent, and Erwin Meijerman of the radiology department at Isala Diaconessenhuis Meppel (the Netherlands) for making their equipment, time, and expertise available for scanning the fossil assemblage. We furthermore thank Nicole Klein for her helpful advice during preliminary assessment and interpretation of the material.

Samenvatting

De voortschrijdende verbetering van tomografische visualisatietechnieken heeft geleid tot een digitale revolutie in paleontologisch onderzoek door de beschikbaarheid van steeds krachtigere hulpmiddelen bij het visualiseren en onderzoeken van fossielen. Hier geven we een beknopt overzicht van de geschiedenis van radiografie en tomografie, bespreken verschillende paleontologische toepassingen van tomografische technieken, en presenteren gepubliceerde voorbeelden waarin tomografische evaluaties hebben geholpen bij de beschrijving en studie van Vossenveld-fossielen. Daarnaast demonstreren we de schadeloze driedimensionale verkenning van fossielen van werveldieren in een micrietmatrix uit de Winterswijkse Steengroeve met behulp van een medische tomograaf. In dit voorbeeld werd de mogelijke aanwezigheid van schedelmateriaal in kalksteenblokken met postcraniaal materiaal van een nog steeds beperkt bekende basale pistosauroïde uit de Vossenveld Formatie onderzocht. Hoewel er geen verborgen skeletelementen in de matrix werden aangetroffen biedt ons onderzoek een heldere illustratie van de tomografische visualisatie van werveldierfossielen in het algemeen, en die uit de Vossenveld Formatie in het bijzonder.

REFERENCES

- **Heijne, J., Klein N., and Sander, P.M. (2019).** *The uniquely diverse taphonomy of the marine reptile skeletons (Sauropterygia) from the Lower Muschelkalk (Anisian) of Winterswijk, The Netherlands. Paläontologische Zeitschrift 93(1), 1-24.*

- **Klein, N., Voeten, D. F. A. E., Lankamp, J., Bleeker, R., Sichelschmidt, O. J., Liebrand, M., Nieweg, D. C. & Sander, P. M. (2015).** *Postcranial material of* Nothosaurus marchicus *from the Lower Muschelkalk (Anisian) of Winterswijk, The Netherlands, with remarks on swimming styles and taphonomy. Paläontologische Zeitschrift, 89(4), 961-981.*

- **Neenan, J.M., Klein, N. & Scheyer, T.M. (2013).** *European origin of placodont marine reptiles and the evolution of crushing dentition in Placodontia. Nature Communications 4: 1621. doi: 10.1038/ncomms2633.*

- **Oosterink, H. W., Berkelder, W., Jong, C. de, Lankamp, J. & Winkelhorst, H. (2003).** *Sauriërs uit de Onder-Muschelkalk van Winterswijk. Nederlandse Geologische Vereniging (ed.): Staringia 11.*

- **Rieppel, O. (2000).** *Sauropterygia I, Encyclopedia of Paleoherpetology, Volume 12A. Verlag Dr. Friedrich Pfeil, München.*

- **Röntgen, Wilhelm K. (1896).** *A new form of radiation. Science 3, no. 72 (1896): 726-729.*

- **Sander, P. M., Klein, N., Albers, P. C., Bickelmann, C., & Winkelhorst, H. (2014).** *Postcranial morphology of a basal Pistosauroidea (Sauropterygia) from the Lower Muschelkalk of Winterswijk, The Netherlands. Paläontologische Zeitschrift, 88(1), 55-71.*

- **Tafforeau, P., Boistel, R., Boller, E., Bravin, A., Brunet, M., Chaimanee, Y., Cloetens, P., *et al.* (2006).** *Applications of X-ray synchrotron microtomography for non-destructive 3D studies of paleontological specimens." Applied Physics A 83(2), 195-202.*

- **Voeten, D. F. A. E., Reich, T., Araújo, R., & Scheyer, T.M. (2018).** *Synchrotron microtomography of a* Nothosaurus marchicus *skull informs on nothosaurian physiology and neurosensory adaptations in early Sauropterygia." PloS One 13, no. 1 (2018): e0188509.*

- **Zuber, M., Laaß, M., Hamann, E., Kretschmer, S., Hauschke, N., Van de Kamp, T., Baumbach, T., & Koenig, T. (2017).** *Augmented laminography, a correlative 3D imaging method for revealing the inner structure of compressed fossils. Scientific Reports 7 (2017): 41413.*

The full list of references can be found at: http://www.geologienederland.nl > Grondboor & Hamer > Staringia 16. De volledige literatuurlijst is te vinden op: http://www.geologienederland.nl > Grondboor & Hamer > Staringia 16.